NASA
Technical Memorandum 107687

ATCOM
Technical Report 92-B-015

Reliability of Stiffened Structural Panels: Two Examples

W. Jefferson Stroud, D. Dale Davis, Jr., Lise D. Maring,
Thiagaraja Krishnamurthy, and Isaac Elishakoff

December 1992

National Aeronautics and
Space Administration

Langley Research Center
Hampton, Virginia 23665-5225

RELIABILITY OF STIFFENED STRUCTURAL PANELS: TWO EXAMPLES

W. Jefferson Stroud
NASA Langley Research Center
Hampton, Virginia

D. Dale Davis, Jr.
Aerostructures Directorate
U.S. Army
NASA Langley Research Center
Hampton, Virginia

Lise D. Maring
Lockheed Engineering and
Sciences Company
Hampton, Virginia

Thiagaraja Krishnamurthy
Analytical Services and
Materials, Incorporated
Hampton, Virginia

Isaac Elishakoff
Florida Atlantic University
Boca Raton, Florida

ABSTRACT

The reliability of two graphite-epoxy stiffened panels that contain uncertainties is examined. For one panel, the effect of an overall bow-type initial imperfection is studied. The size of the bow is assumed to be a random variable. The failure mode is buckling. The benefits of quality control are explored by using truncated distributions. For the other panel, the effect of uncertainties in a strain-based failure criterion is studied. The allowable strains are assumed to be random variables. A geometrically nonlinear analysis is used to calculate a detailed strain distribution near an elliptical access hole in a wing panel that was tested to failure. Calculated strains are used to predict failure. Results are compared with the experimental failure load of the panel.

INTRODUCTION

Although a probabilistic analysis provides more information than the corresponding deterministic analysis, a probabilistic analysis also *requires* more information, namely, the joint probability densities of the random variables. In addition, a probabilistic analysis requires substantially more computations than the corresponding deterministic analysis. For the most part, prior to the mid-1970's, the additional information provided by a probabilistic structural analysis was not thought to be worth the additional effort and expense. Now, however, there is substantial evidence that that position is changing. That evidence includes the increasing number of reliability-oriented specialty conferences, short courses, sponsored research, research papers, and technical books. There is also an increased interest in reliability-based design codes, such as codes for naval and commercial ships and offshore structures.

One reason for the increased acceptance of probabilistic structural analysis is that the solutions to many classes of deterministic problems are becoming routine; such solutions are required in order to solve the corresponding probabilistic problem. Another reason is that probabilistic computations are becoming easier and less expensive because useful software is being developed (e.g., SwRI, 1991 and Olesen, 1992), and adequate computers are readily available to most users. A third reason is that probabilistic methods, and the information these methods provide, are becoming more widely understood (e.g., Liu and Belytschko, 1989) and better appreciated (e.g., Chamis, 1986).

In an effort to increase that understanding and appreciation, this paper examines the performance of two composite stiffened panels from the point of view of reliability, which is the probability that the panels can carry a specified load without failure. Failure mechanisms considered are buckling and excessive strain. This paper focuses on results and does not address methods.

Two types of example applications are examined. They are distinguished by the random variables involved in calculating the reliability. In one example, the random variable is the size of an overall bow-type initial imperfection in a panel which is designed assuming that it is flat. The bow is in the shape of a half-sine wave along the length of the panel. The reliability is calculated for several probability density distributions of the size of the initial imperfection. In the other example, the random variables are the allowable strains. In this case, a geometrically nonlinear analysis is used to calculate detailed strains near an elliptical access hole in a wing panel that was tested to failure. Using these calculated strains, the reliability of the panel is calculated for several probability density distributions of the allowable strains and for several definitions of panel failure, all of which are based on excessive strain at the ply level. Results are compared with the experimental failure load of the panel.

EFFECT OF BOW-TYPE INITIAL IMPERFECTION ON RELIABILITY

In this first example application, a square graphite-epoxy blade-stiffened panel is designed to carry combined in-plane compression and shear. The panel is designed as if it had no initial imperfection – that is, as if it were perfectly flat. Optimization techniques are used to produce a minimum-weight design. The panel produced by the optimization is analyzed assuming that it has an overall bow-type imperfection. Then the size of the bow is taken to be a random variable with several specified statistical distributions. The reliability of the panel is calculated at various loads for each assumed distribution of the size of the bow. The objectives are: (1) to establish the effect of a bow-type imperfection on the reliability of stiffened panels and (2) to assess the sensitivity of the reliability to accurate specification of bow statistics. For this first problem, all structural analysis and structural design are carried out with the computer program PASCO (Anderson et al., 1980). Probabilistic calculations are carried out with simple, special-purpose computer programs. This first example, which is part of a broader analytical study, is described in detail by Stroud et al. (1992).

Panel Configuration

The graphite-epoxy panel contains six equally-spaced blade stiffeners, is 30 in. long, and is 30 in. wide. The overall shape and loading are shown in figure 1. The skin, blade, and attachment flanges are balanced, symmetric laminates containing $\pm 45°$, $0°$, and $90°$ plies. In the optimization, the design variables are the various ply thicknesses and the depth of the blade. The design load is combined compression and shear with $N_x = 3000$ lb/in and $N_{xy} = 1000$ lb/in. Although inequality constraints are placed on buckling and ply-level in-plane strains, only the buckling constraint affects the final design. A repeating element of the final design is shown in figure 2.

Effect of Initial Bow on Buckling Load

The minimum-weight panel described above is analyzed assuming that it has various amounts of initial bow. The bow is in the form of a half-sine wave along the length (fig. 3). The size of the bow at panel midlength is denoted e. When the panel is in compression, the bow causes large bending strains which are added to the uniform axial strains of the perfect panel. A positive value of e adds compression to the skin, and a negative value of e adds compression to the tips of the blades. The failure load of the panel is assumed to be the lower of (1) the buckling load and (2) the load at which strains exceed specified ply-level allowables. For this panel, buckling always occurs at the lower load.

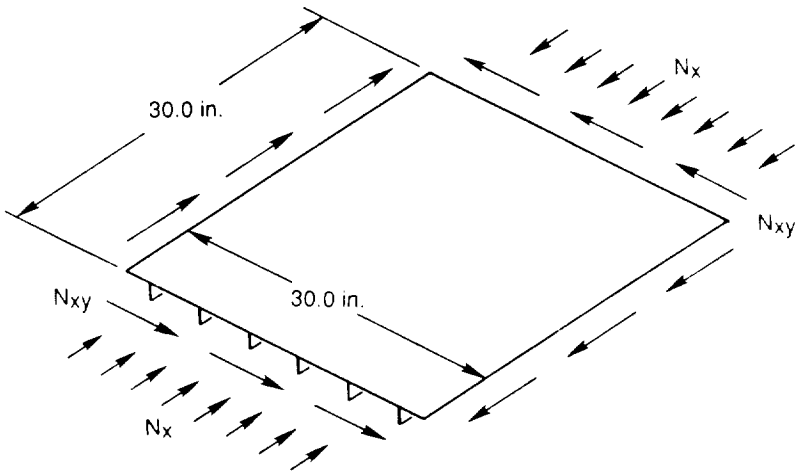

Figure 1. Overall shape and loading for square, blade-stiffened panel designed herein. The panel is designed as if it were flat.

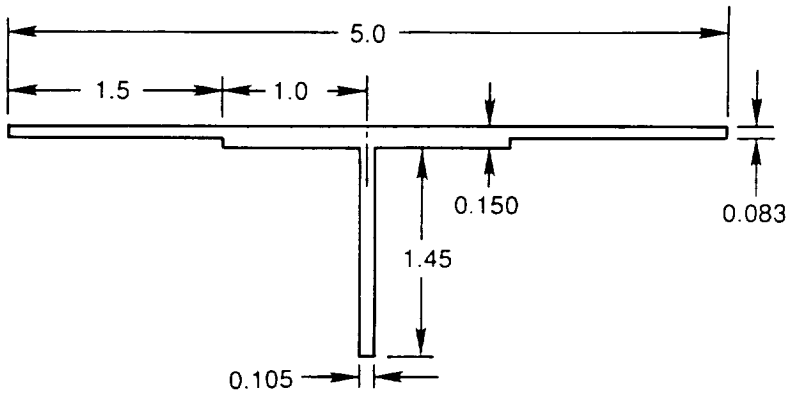

Figure 2. Final design for square, blade-stiffened panel. One repeating element is shown. Dimensions are in inches.

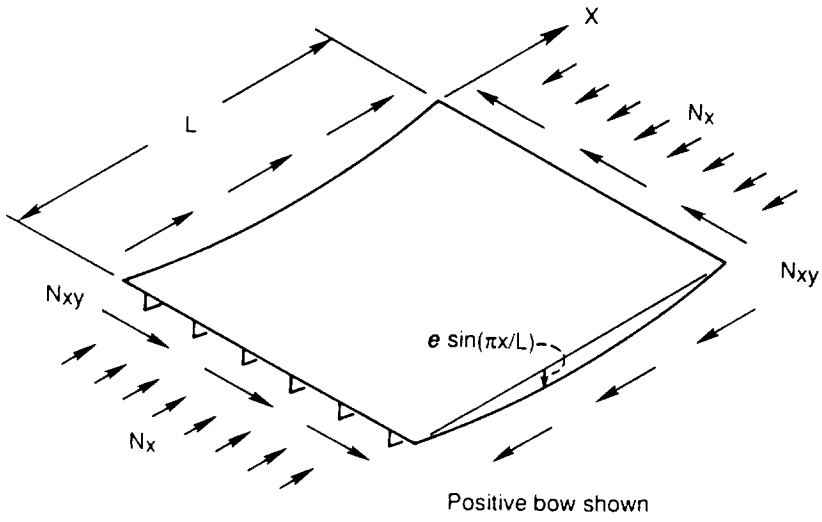

Figure 3. Stiffened panel with initial bow and applied loading.

In figure 4, the ratio of the failure load to the design load is shown as a function of e. Note that the curves are not symmetric with respect to the line $e = 0.0$. A negative bow reduces the failure load more than does a positive bow. For example, at e = -0.1 in. the panel buckles at about 57% of the design load. Both components of the design load vector are multiplied by the same factor to obtain the failure load vector, as shown in equation 1.

$$\begin{bmatrix} N_x \\ N_{xy} \end{bmatrix}_{failure} \approx 0.57 \begin{bmatrix} N_x \\ N_{xy} \end{bmatrix}_{design} = 0.57 \begin{bmatrix} 3000 \\ 1000 \end{bmatrix} = \begin{bmatrix} 1710 \\ 570 \end{bmatrix} \tag{1}$$

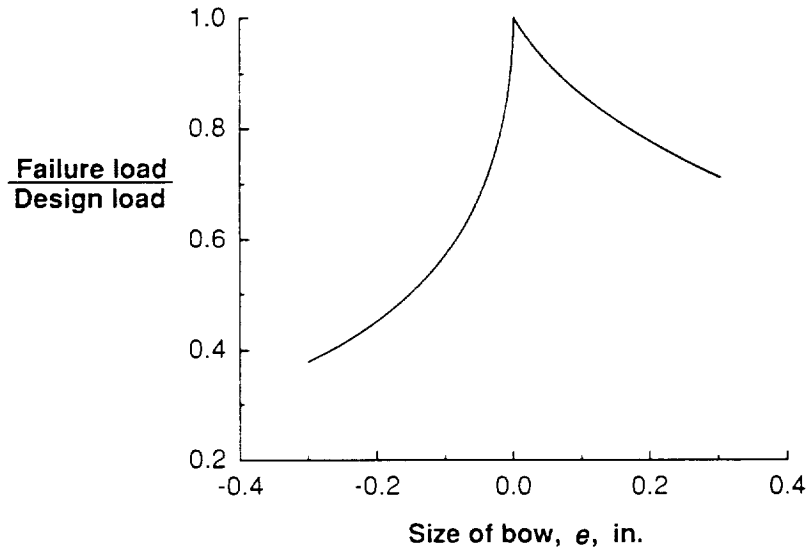

Figure 4. Variation of nondimensional failure load with initial bow for square, blade-stiffened panel. For this case, the failure load is the buckling load.

Reliability

The reliability of a structure is defined as the probability that the structure will perform its intended function without failing. In the present context, the reliability is the probability that the panel will carry a given load without buckling. To calculate the reliability, two types of information are needed: (1) the relationship between the failure load of the panel and the possible values of the random variables, and (2) the joint probability density of the random variables.

In this example, there is a single random variable – the size e of the bow. The first type of information, the failure load as a function of e, is obtained using PASCO and is illustrated in figure 4. In subsequent sections of this paper, e is assumed to have various, specified probability densities. This assumption provides the second type of information.

In the first section below, three different distributions of e are examined – a normal distribution and two extreme value distributions – all with the same mean and the same standard deviation. In the second section, the distributions are similar to those in the first section, except that the distributions are truncated; a value of e larger than a specified value is not allowed. Studies are presented which show the effect of these distributions on the reliability of the panel.

Bow with Normal and Extreme Value Distributions. In this section, a comparison is made between the reliabilities of panels having three different distributions for the size of the bow – a normal distribution, a Type I Asymptotic Distribution of Maximum Extreme Values (maximum extreme value distribution), and a Type I Asymptotic Distribution of Minimum Extreme Values (minimum extreme value distribution)[1]. Parameters defining the three distributions are selected so that all three distributions have the same mean and the same standard deviation (μ = 0.0 in. and σ = 0.02 in., respectively). Only the higher statistical moments differ. The probability density functions for the three distributions are shown in figure 5.

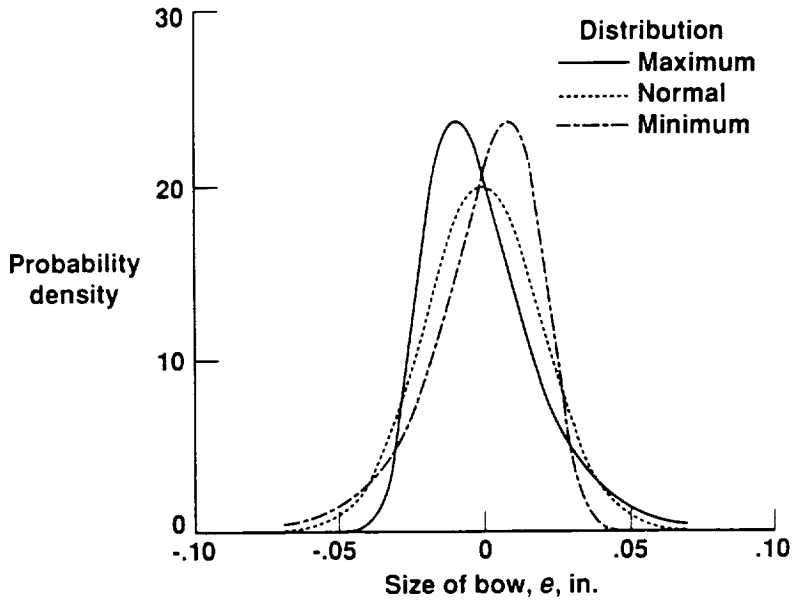

Figure 5. Probability densities for three distributions of the bow: maximum extreme value, normal, and minimum extreme value. Each distribution has a mean of zero and a standard deviation of 0.02 inch.

The reliability of the imperfect panel at various load levels is presented in figures 6 and 7. The entire load range is shown in figure 6 and only the high-reliability portion of the load range is shown in figure 7. (For reference, the reliability of a perfectly flat panel is also shown in figure 6.) At low load levels (Applied load/Design load $\leq$ 0.55) the reliability is approximately unity for the imperfect panel, regardless of the distribution of the size of the bow. For higher load levels, the reliability decreases and depends upon the distribution of the size of the bow. When the applied load is equal to the design load, the reliability is zero.

---

[1] Extreme value distributions are important distributions for engineering applications. These distributions can be used to describe the maximum or minimum values exhibited by random phenomena such as wind speed, wave heights, and rain fall. The phenomena have distributions, but it is only the maximum or minimum values of the phenomena that are of interest – not the average or typical values. If a phenomenon has a distribution with an exponentially-decaying tail in the direction of interest (to the right is maximum, etc.), the corresponding extreme value distribution is denoted Type I. A normal distribution is an example of a distribution with exponentially-decaying tails in both directions.

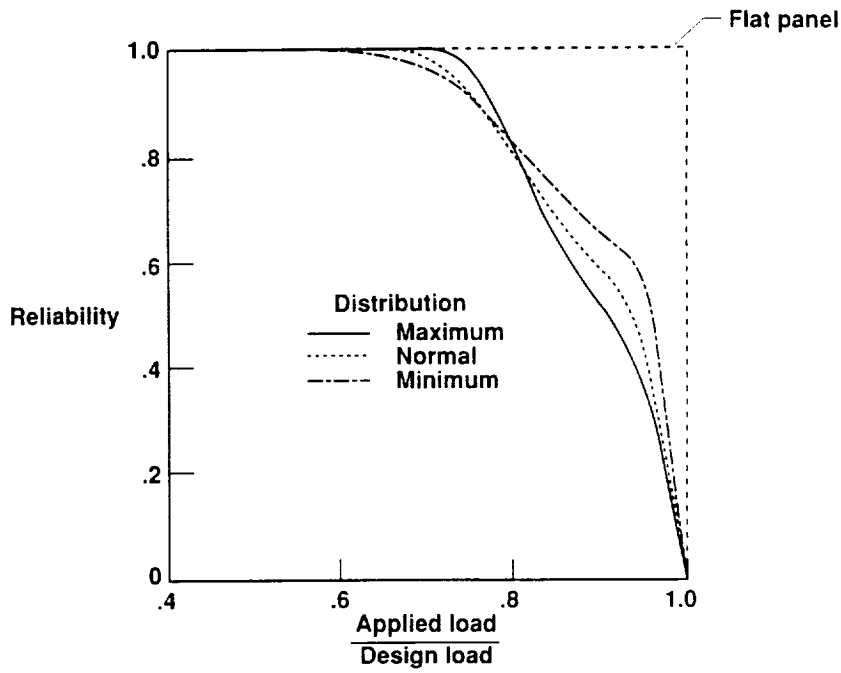

Figure 6. Reliability of square, blade-stiffened panel versus ratio of applied load to design load, for three distributions of the bow. The probability densities for these three distributions are given in figure 5. Reliability of perfectly flat panel is also shown.

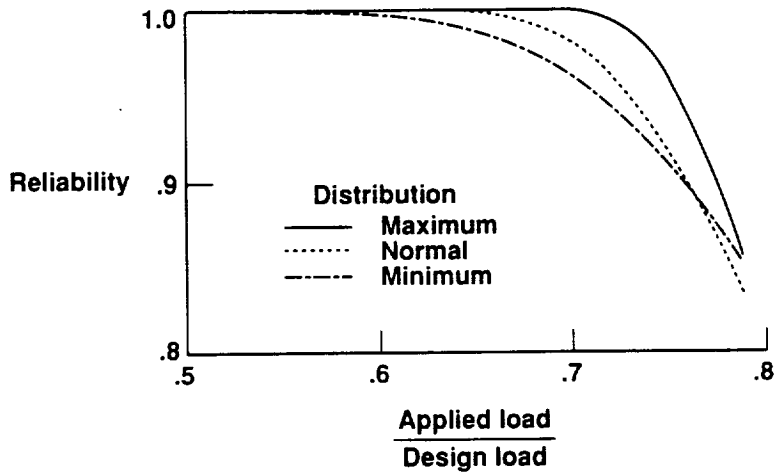

Figure 7. Reliability of square, blade-stiffened panel versus ratio of applied load to design load. Results are shown near reliability = 1.0 for three distributions of the bow. The probability densities for these three distributions are given in figure 5.

The reliability curves in figures 6 and 7 illustrate the imperfection sensitivity of the panel and, hence, the importance of accounting for a bow when designing a panel. For example, for a normal distribution, to obtain a reliability of 0.999, the load must be reduced to about 65% of the design load. This means that to obtain a reliability of 0.999, a designer could "ignore" the imperfection, but, instead, use a safety factor of about $1/.65 \approx 1.5$. However, this safety factor would account for the uncertainty of only this bow-type initial imperfection. Other uncertainties would not be accounted for.

In addition, there are substantial differences between the curves, even though the means and standard deviations of the imperfections are equal. These differences demonstrate that the reliability of an imperfect panel depends upon the details of the probability density of the imperfection. The results can be interpreted in the following two ways.

First, suppose that there are three panel fabrication processes and that imperfection data collected on these three processes have the same mean and the same standard deviation. The results indicate that, with this limited data, it would be inaccurate to assume that the three fabrication processes are equivalent. Since the distributions could differ, one of the processes could produce panels that are considerably more (or less) reliable than the other two processes.

Second, suppose that there is only one fabrication process and that only the mean and the standard deviation are known. To make calculations defining the performance of the panels, it is necessary to assume the distribution of the imperfection – which means that the higher statistical moments are assumed. The results indicate that the calculations will be very sensitive to the assumptions. Moreover, the common assumption of a normal distribution can be either conservative or unconservative.

Bow with Truncated Normal and Truncated Extreme Value Distributions. In practice, quality control procedures would eliminate panels that have a bow larger than a specified maximum value. For that reason, the large tails on the probability density functions (e.g., fig. 5) are unrealistic. Using truncated distributions is one way to study panel reliability and, at the same time, account for such quality control measures.

In this section, the distributions of the bow are similar to those of the previous section, except that the distributions are truncated. For these studies, the absolute value of the maximum bow (e_{max}) is selected to be 0.04 in. Since the standard deviations (σ) of the original untruncated distributions are 0.02 in., the maximum bow is $\pm 2\sigma$ of the original, untruncated distributions. The probability density functions for these distributions are shown in figure 8.

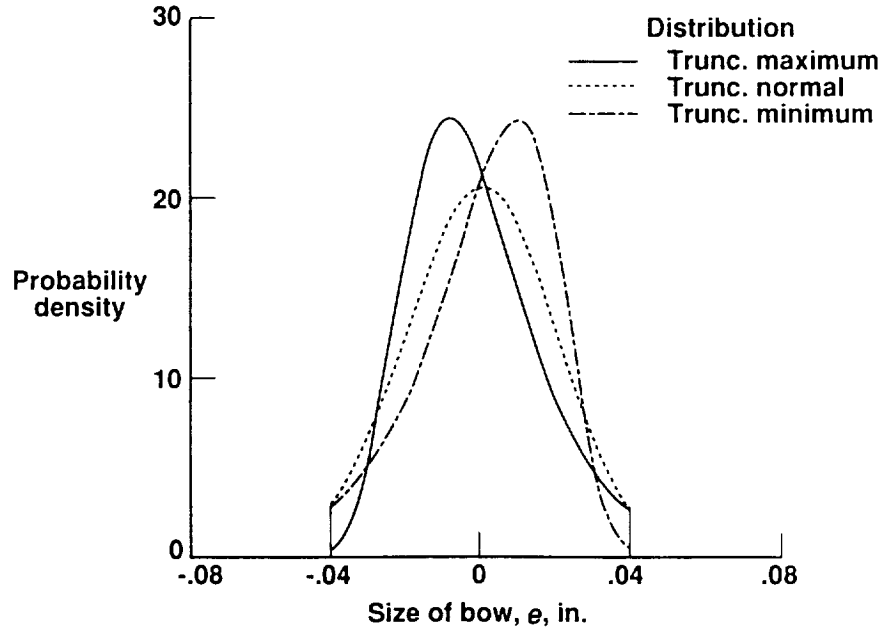

Figure 8. Probability densities for three truncated distributions. Original probability densities (maximum extreme value, normal, and minimum extreme value) are given in figure 5. Truncations occur at $e = \pm 0.04$ inches.

The reliability of the panel with these distributions of e is shown in figure 9. For comparison, the figures also include the reliability of the panel if the distributions are not truncated.

The results indicate that if the original distribution is minimum extreme value, an e_{max} of $\pm 2\sigma$ provides a substantial increase in reliability. If the original distribution is normal, an e_{max} of $\pm 2\sigma$ provides a moderate increase in reliability. If the original distribution is maximum extreme value, an e_{max} of $\pm 2\sigma$ has negligible effect on panel reliability.

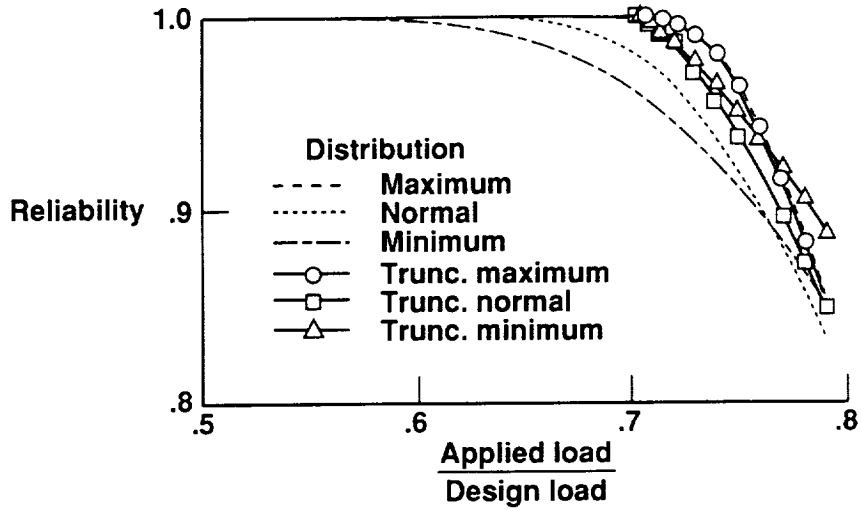

Figure 9. Reliability of square, blade-stiffened panel for original and truncated distributions of figures 5 and 8, respectively.

The differences between the three cases cited above are caused by the interaction between the shape of the curve that defines the failure load as a function of e (fig. 4) and the shapes of the various distributions of e (figs. 5, 8). For the minimum extreme value case, truncating the distribution removes a large tail extending to the left ($e < .04$ in.). For this case, there is a substantial increase in reliability of the remaining panels because panels with the lowest buckling loads are removed, as can be seen in figure 4. However, for the maximum extreme value case, truncating the distribution removes a large tail extending to the right ($e > .04$ in.). For this case, there is no increase in reliability because panels with only a moderate reduction in buckling load are removed.

This last example illustrates that some imperfections are more important than others, and that if quality control removes only the less important imperfections it is accomplishing very little. The results also indicate that even with truncated distributions, the reliability is sensitive to details of a distribution – but much less sensitive for the truncated distribution than for the untruncated distribution.

EFFECT OF ALLOWABLE STRAINS ON RELIABILITY

In the second example application, a rectangular graphite-epoxy I-stiffened panel similar to a panel on the wing of the V-22 tiltrotor aircraft (fig. 10) is analyzed using a geometrically nonlinear analysis. The loading is uniaxial compression in the direction of the stiffeners. Ply-level strains are calculated near an elliptical access hole to examine possible failure mechanisms. (Prior to this paper, the panel was tested to failure.) These calculated strains are compared with allowable strains in a failure criterion based on maximum strain. The allowable strains are the random variables in the reliability analysis.

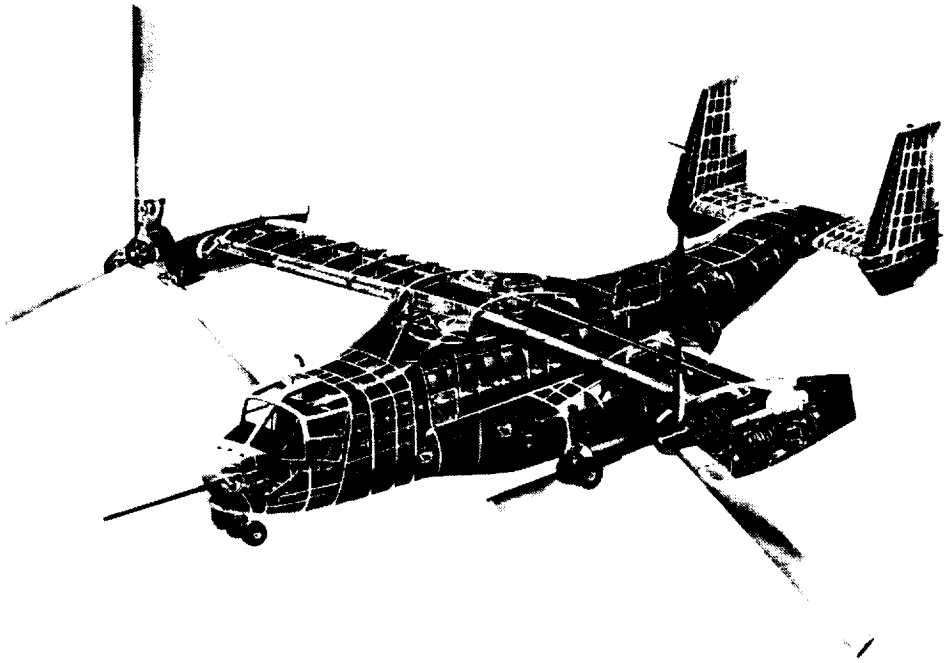

Figure 10. V-22 tiltrotor aircraft.

The panel's reliability is calculated for several distributions of the allowable strains and for several variations of the failure criterion. Results are compared with the experimental failure load of the panel. For this second example, all structural analyses are carried out with the computer program COMET (Stewart, 1989); all probabilistic computations are carried out with the computer program NESSUS (SwRI, 1991). More complete descriptions of the panel and of the analysis are presented by Davis (1991).

Description of Panel

The graphite-epoxy test panel is 35 inches wide by 78 inches long and has five I-shaped stiffeners. An illustration of the panel showing the various components and regions of interest is shown in figure 11. Figure 12 is a photograph of the panel. As can

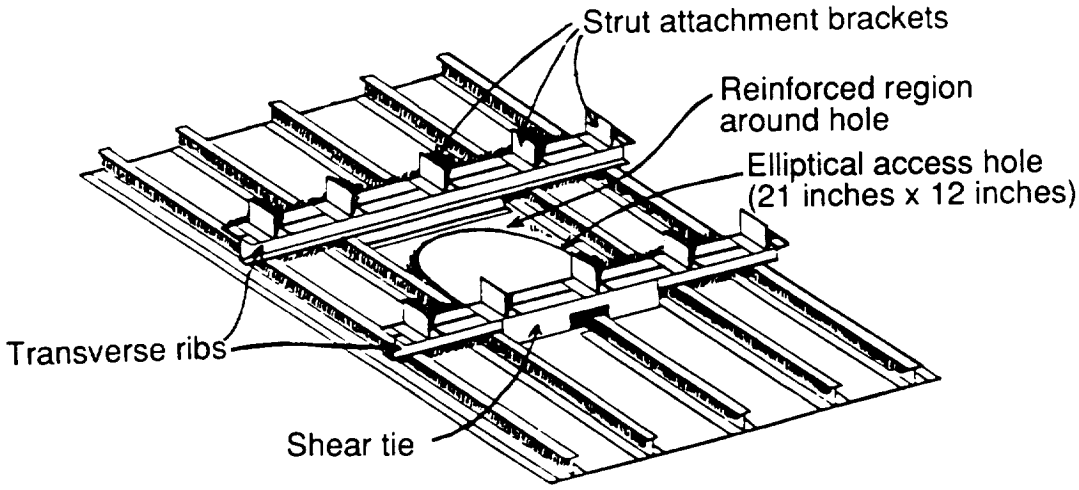

Figure 11. Sketch of test panel illustrating key components.

be seen in figures 11 and 12, the center stiffener is discontinuous due to the presence of an elliptical access hole. The access hole is large enough (12 in. by 21 in.) for a person to visually inspect the interior of the wing. This panel is a major structural component having a design ultimate compression load of 334,000 pounds (334 kips) in the direction of the stiffeners. The design limit compression load is 260 kips. In addition to design requirements on strength, there are design requirements on stiffness and damage tolerance.

Figure 12. Photograph of test panel.

The skin beneath the stiffeners is padded up by interleaving 0° plies into the skin. The region surrounding the access hole is padded up with ±45° plies. These ±45° plies help transfer the load around the access hole to the adjacent stiffeners. A complex system of graphite-epoxy and metallic test fixtures are attached to the panel at each end of the access hole. During testing, these fixtures were attached to struts (fig. 13) which restrained lateral deflection and simulated the bulkhead-type transverse ribs of the aircraft wing box. The analysis is intended to simulate the test.

Analysis

The finite element model[2] that is used to analyze the panel is shown in figure 14. A top view showing a close-up of the center portion containing the access hole is also shown in figure 14. The finite element is a 9-node assumed natural-coordinate strain (ANS) shell element, denoted EX97 within COMET, the structural analysis code that is used to perform the analysis. The model contains 2284 elements, 9486 nodes, and 47,304 degrees-of-freedom. Forty-six different laminates are used to model the panel.

[2] The validity of the finite element model was checked several ways. The final finite element model was developed by using a sequence of models of increasing complexity. In the early stages of model development, the models were validated by making comparisons with PASCO results that were known to be accurate. In the final stages, where independent results were not available, comparisons were made between results obtained using variations of the finite element model. Finally, error analysis techniques were applied.

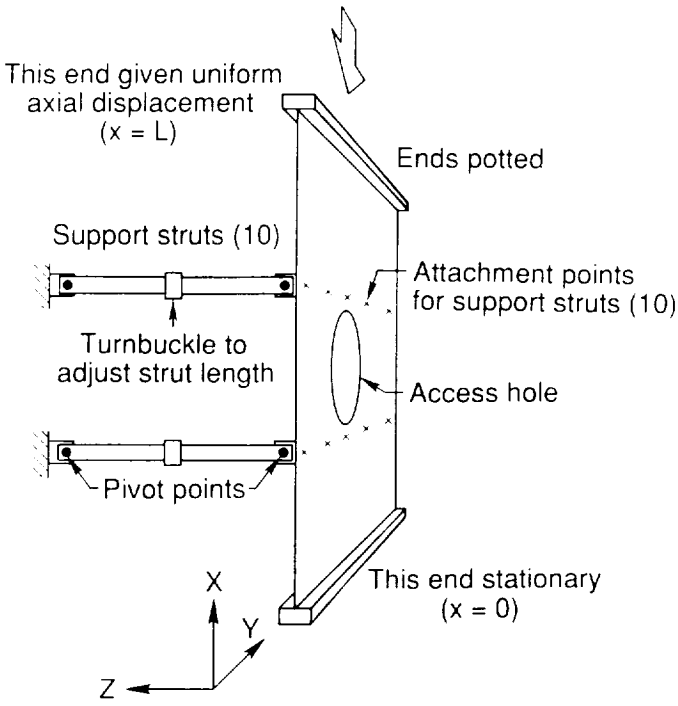

Figure 13. Schematic of test panel in test apparatus.

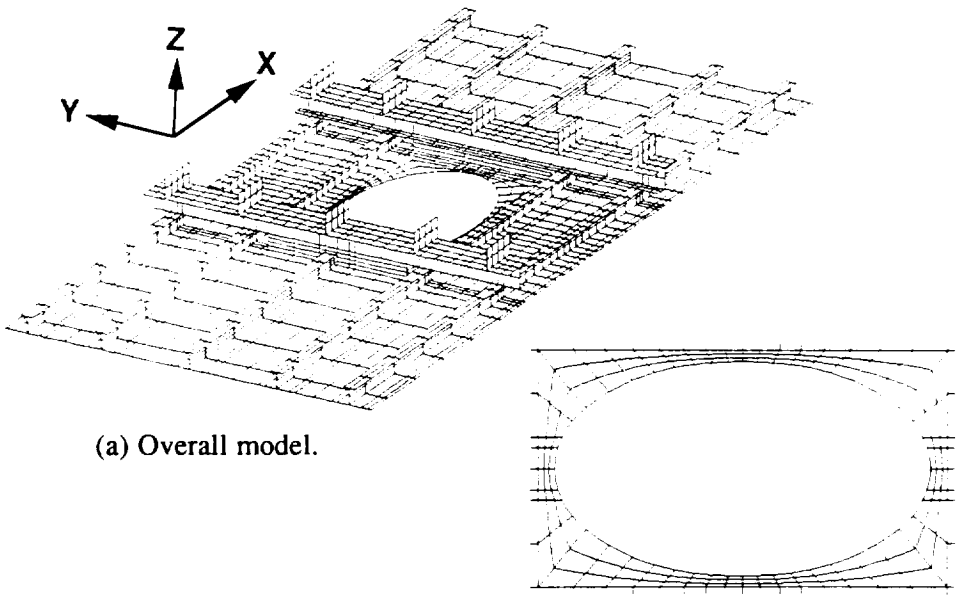

(a) Overall model.

(b) Top view, close-up of center portion of model, near elliptical access hole.

Figure 14. Finite element model of V-22 panel.

To simulate the effects of the support struts shown in figure 13, boundary conditions are specified for the nodes at the midpoint of the top of the strut attachment brackets. At these ten points, displacements in the z-direction and rotations about the X-axis are set to zero, while rotations about the Y-axis are free (to simulate the pins that attach the struts to the attachment brackets). Since both ends of the panel are potted, thus virtually clamping the ends, all degrees-of-freedom at $x = 0$ and $x = L$ are set to zero, except for the displacement in the x-direction at $x = L$, where uniform end-shortening is specified to simulate the crosshead motion of the testing machine.

A geometrically nonlinear analysis is used to calculate in-plane strain components in each composite ply of each finite element. These strains are used in the failure analysis.

Analysis Results & Test Correlation

Nonlinear Analyses. A deformed geometry plot for the nonlinear analysis is shown in figure 15. The out-of-plane deformation at the edge of the access hole is substantially greater for this nonlinear analysis than for the corresponding linear analysis (Davis, 1991).

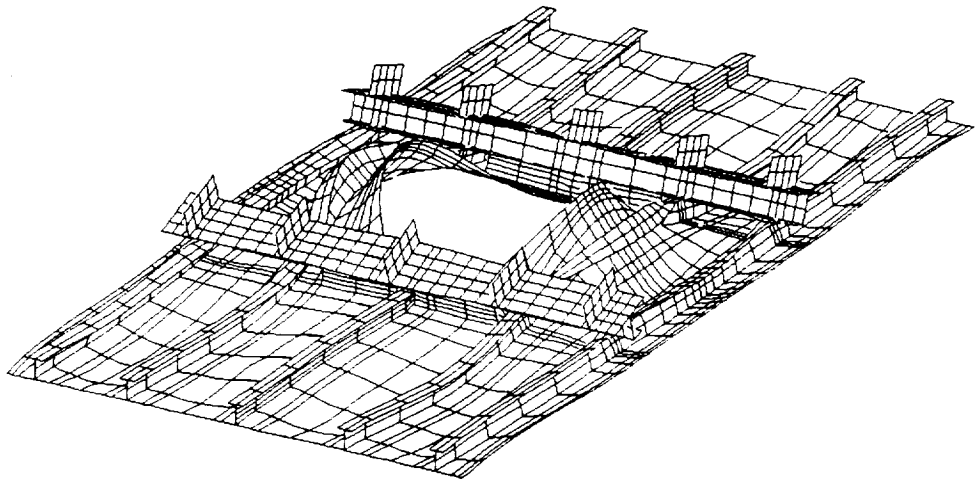

Figure 15. Deformed geometry obtained using geometrically nonlinear analysis.

The element midplane strains and curvatures are used to calculate the strains on the top and bottom surfaces of the structural material. The axial strains at the top and bottom surfaces of the skin at the edge of the access hole are plotted as a function of applied load in figure 16. The open circles represent discrete load steps from the nonlinear analysis, the dashed lines represent the extension of the linear path, and the filled symbols represent strain gage data. The vertical line at 405 kips indicates the load at which the test panel failed. At a given load, the differences in the strains on the top and bottom surfaces are caused by bending. The axial strains at the edge of the access hole are the highest axial strains in the panel.

In general, there is excellent agreement between the strain gage data and the results from the nonlinear analysis. Although the linear analysis correlates well at the lower loads, the nonlinear analysis is necessary to predict the complicated response of the panel as it approaches the failure load.

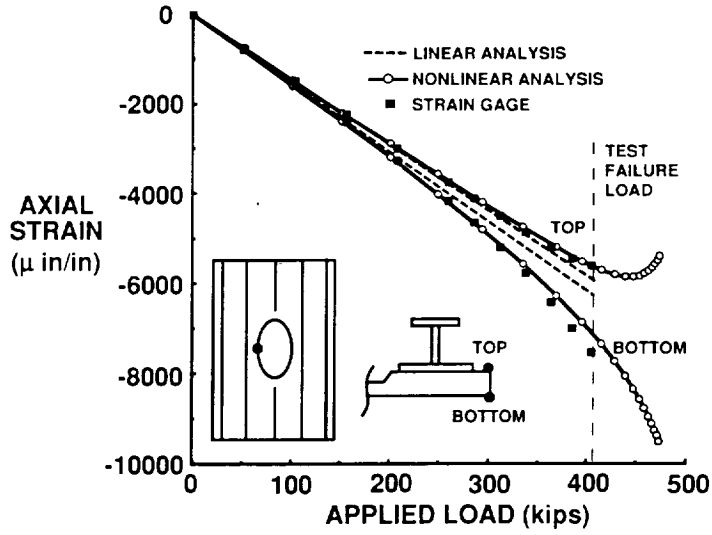

Figure 16. Axial strain as a function of applied load. Locations are at top and bottom of skin at edge of access hole.

Failure Analysis. In-plane, ply-level strains calculated in the nonlinear analysis are used to perform a failure analysis of the panel. Because the highest strains are in the unstiffened region near the elliptical access hole, that region is examined in the failure analysis. The laminate in that region contains 46 plies.

The failure criterion is maximum strain at the ply level. A ply is assumed to fail when any strain component in that ply exceeds the corresponding allowable strain. Panel failure is assumed to occur when there is failure of a specified percentage of plies in any finite element. In the studies presented herein, the specified percentage of plies that defines panel failure is varied from 2.2% (one ply fails) to 40% (18 plies fail). The failure analysis is not progressive – that is, the failure analysis does not reduce the stiffness of the failed plies or redistribute the load. The ply-level allowable strains are the random variables in the reliability analysis. The mean values of the ply-level allowable strains are given in Table I.

Table I. Mean values of in-plane, ply-level allowable strains.

ε_{1t}	=	.00829	Subscripts:
ε_{1c}	=	-.00829	1 - fiber direction
ε_{2t}	=	.00388	2 - transverse to fibers
ε_{2c}	=	-.02388	t - tension
γ_{12}	=	.00948	c - compression

Based on the stress and failure analyses, the elements that are first to fail are indicated in figure 17. The elements are at a small angle to the minor axis of the ellipse. A photograph of the center portion of the panel after testing is shown in figure 18. A failure crack passes through the region predicted by the analysis. The predicted failure mode is excessive shear strain.

It is emphasized that a failure criterion is *assumed*. No attempt is made here to develop or advocate a failure criterion.

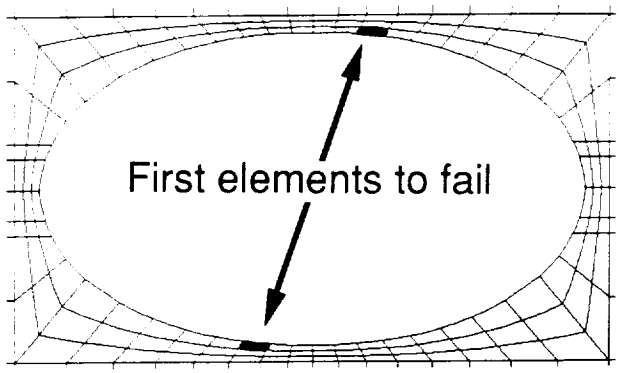

Figure 17. Finite element mesh near access hole. Finite elements that are first to fail are indicated.

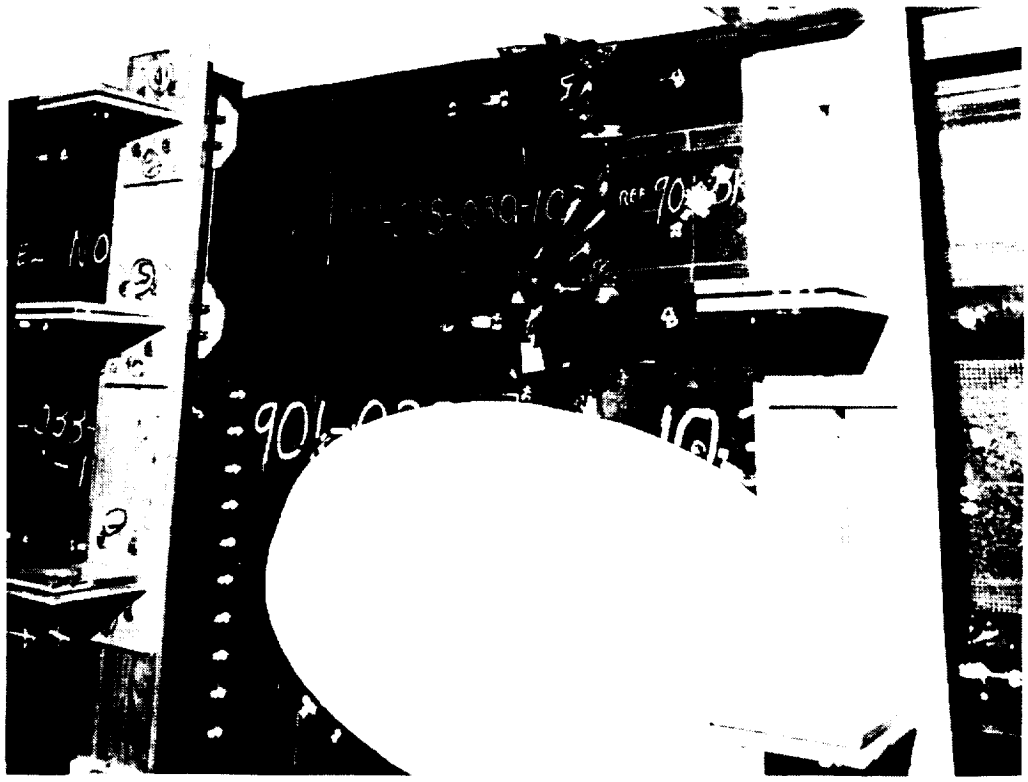

Figure 18. Photograph of failed test panel in region around access hole.

Reliability

The panel's reliability is calculated with NESSUS using a Monte Carlo simulation with 10,000 realizations. (Several calculations were checked using 50,000 realizations; differences were minor.) The allowable strains are assumed to be independent random variables with normal distributions and with mean values given in Table I. Two parameters are varied: (1) the coefficient of variation of the allowable strains and (2) the percentage of failed plies that defines panel failure. Results in terms of the panel's reliability as a function of applied load are presented in figures 19 and 20. The data are given at the discrete load steps for the nonlinear analysis. The coefficient of variation is denoted COV and is defined as the ratio of the standard deviation to the mean, expressed as a percent. That is, $COV=\sigma/\mu \times 100\%$.

In figure 19, COV of the allowable strains is fixed at 5%, and the percentage of failed plies that defines panel failure varies between 2.2% and 40%. For loads equal to or less than 335 kips, the reliability is 1.0 regardless of the percentage of failed plies that defines panel failure. This means that the panel is highly reliable at the design ultimate load of 334 kips. At higher loads, the reliability becomes smaller and depends upon the percentage of failed plies that defines failure. At an applied load of 395 kips, the reliability varies from 0.30 (failure of 2.2% of the plies in an element defines panel failure) to 0.83 (failure of 40% of the plies in an element defines panel failure). Recall that the 2.2% criterion means that failure of a single ply defines panel failure.

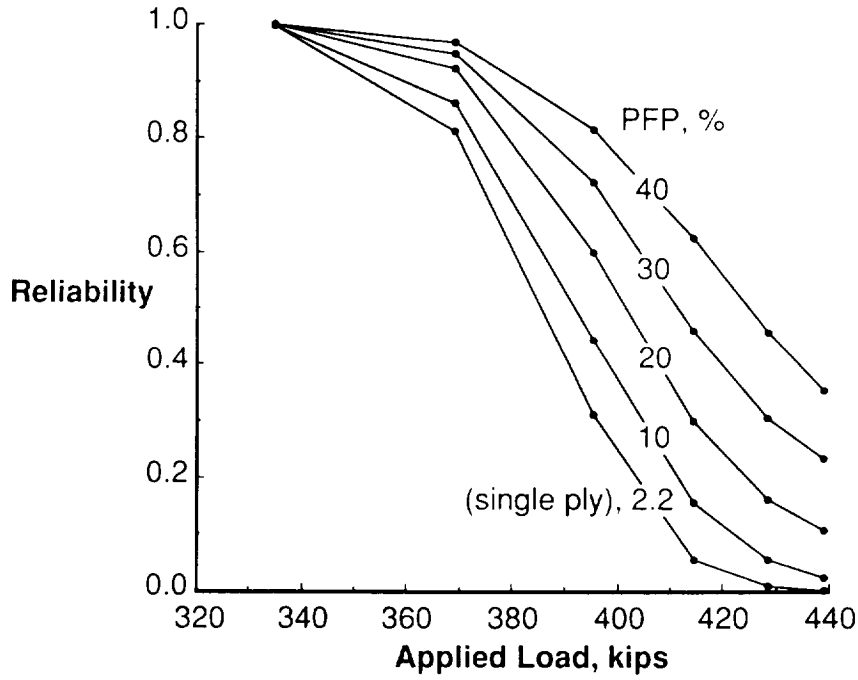

Figure 19. Reliability of panel as a function of applied load. Coefficient of variation of allowable strains is fixed at 5%. Results are for several values of percentage of failed plies (PFP) that defines panel failure.

In figure 20, the percentage of failed plies that defines panel failure is fixed at 20%, and COV varies from 0.0 to 10%. For the case COV = 0.0, which is the traditional deterministic analysis, the analysis predicts a failure load of 403 kips compared with a test failure load of 405 kips. That, of course, is excellent agreement. However, for COV=5%, which is a reasonable value, the same postulated failure criterion predicts that panel failure can occur over a broad range of loads, as indicated in figure 21. The height of the bars in figure 21 indicates the likelihood of the panel failing in a given load range. For example, there is a 30% chance that the panel will fail in the range 395–415 kips. There is also an 11% chance that the panel will fail at a load greater than 439 kips. Because accounting for uncertainties in allowable strains produces a broad range of possible failure loads, and because accounting for additional uncertainties (always present) produces an even broader range of possible failure loads, a highly accurate (within 5 percent) prediction of the failure load of the composite panel is unlikely. The excellent agreement mentioned above is fortuitous.

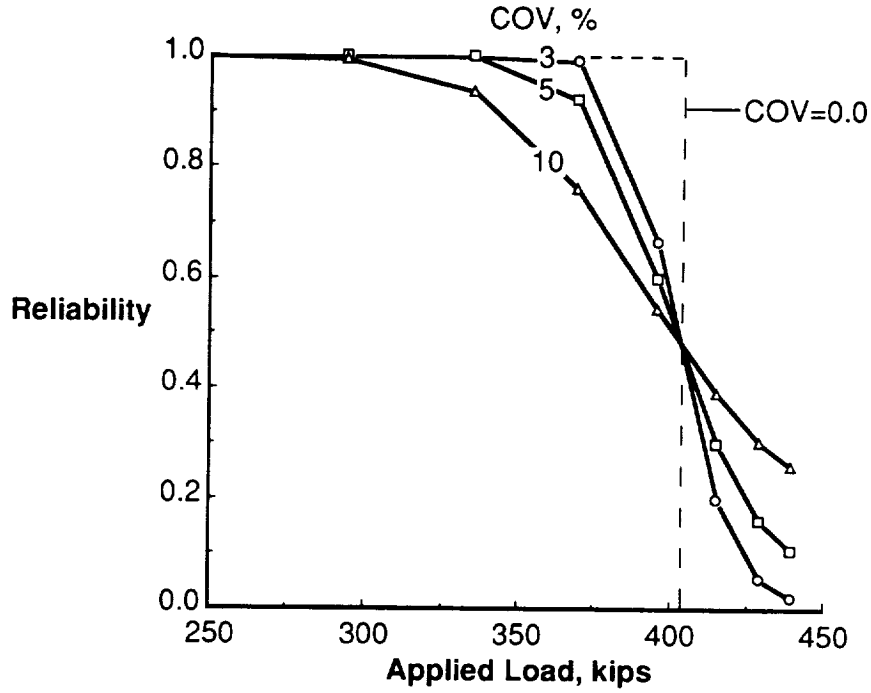

Figure 20. Reliability of panel as a function of applied load. Percentage of failed plies that defines panel failure is fixed at 20%. Results are for several values of the coefficient of variation (COV) of allowable strains.

Probabilistic analysis helps to demonstrate and explain the difficulty in predicting the failure load of a structure. A highly accurate prediction requires *both* an excellent mathematical model (including a valid failure criterion) and low variability of important parameters (including material properties, dimensions, support conditions, and loads). If the variability of important parameters is not low but can be modeled, then the reliability of the structure can be calculated. However, in that case, the failure load of a particular structure is unlikely to be predicted with high accuracy.

CONCLUDING REMARKS

Analytical studies are carried out on two graphite-epoxy stiffened panels to determine the effect that certain parameters have on the reliability of a panel.

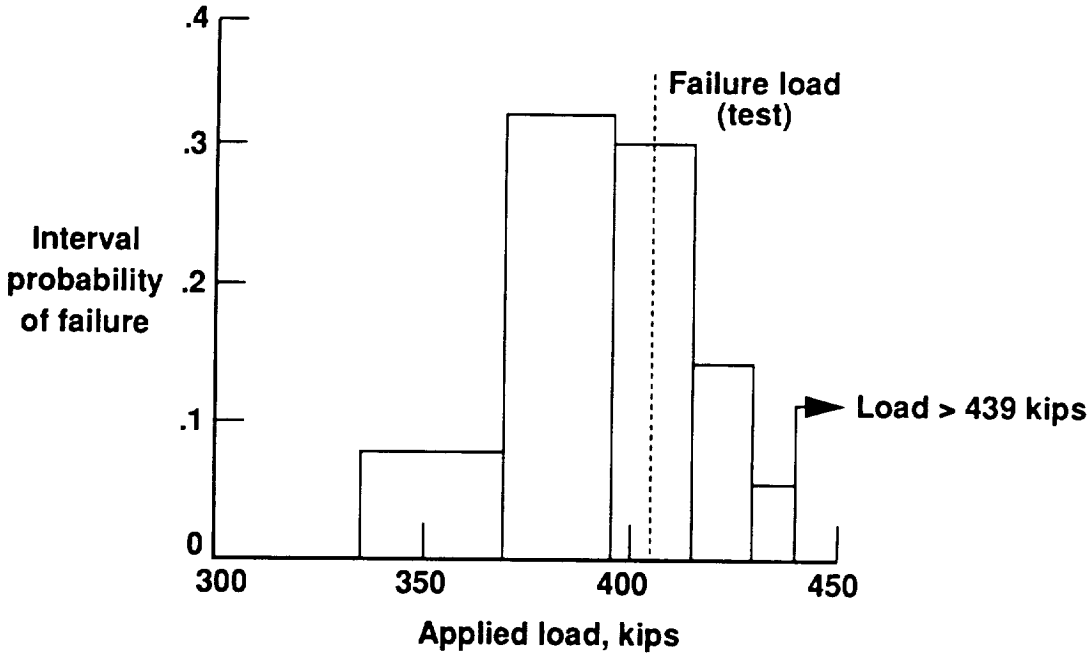

Figure 21. Probability of failure over various load ranges. Coefficient of variation of allowable strains is 5%. Percentage of failed plies that defines panel failure is 20%. Arrow indicates failure probability (0.11) for a load greater than 439 kips.

The first panel is a minimum-weight panel that is designed as if it were perfectly flat. The loading is combined in-plane compression and shear. The objective of the study is to determine the extent to which a small overall bow-type initial imperfection can degrade the panel's reliability. The bow is in the shape of a half-sine wave down the length of the panel. The random variable is the size of the bow. The degradation caused by the initial imperfection is found to be substantial. For a panel having a bow with a normal distribution with mean of zero and standard deviation of 0.02 in., to obtain a reliability of 0.999 the applied load must be reduced to about 65% of the design load of the perfect panel. This means that to obtain a reliability of 0.999, a designer could ignore the imperfection, but, instead, use a safety factor of about $1/.65 \approx 1.5$. However, this safety factor would account for the uncertainty of only this bow-type initial imperfection.

To determine the sensitivity of the reliability to details of the bow statistics, studies are made with three distributions of the size of the bow. All three distributions have the same mean and same standard deviation. The three distributions are: (1) normal, (2) maximum extreme value, and (3) minimum extreme value. Although the probability density functions have the same general shape, the panel reliabilities are quite different. These differences indicate that the reliability is sensitive to the details of the bow distribution. This sensitivity should be taken into account when making assumptions regarding the probability density of the bow and when selecting a fabrication process.

Good quality control would eliminate panels with a bow larger than a specified maximum value. To examine the effect of quality control, panel reliability is studied for bows having truncated distributions. The basic distributions are the same as the three types mentioned above. For two distributions (minimum extreme value and normal), truncating the distributions causes the reliability to improve; for the remaining distribution (maximum extreme value) the reliability is unchanged. The maximum extreme value case illustrates that some imperfections are more important than others, and that if quality control removes only the less important imperfections it is accomplishing very little. The reliability is less sensitive to the probabilistic details of the imperfection when the distributions are truncated.

The second panel is similar to a wing panel in the V-22 tiltrotor aircraft. The loading is in-plane uniaxial compression. In-plane strains are calculated using a geometrically nonlinear finite element analysis. These strains are used to perform a failure analysis based on maximum strain at the ply level. The random variables are the values of the allowable strains. The objective of the study is to determine the extent to which uncertainties in allowable strains affect the panel's reliability. Results from the reliability analysis are compared with the experimental failure load of the panel.

Using a deterministic approach and a postulated failure criterion, the predicted failure load and the experimental failure load are in close agreement (about 1% difference). However, the comparison becomes more realistic when the analysis accounts for a reasonable variation in the allowable strains. With that variation, the same stress analysis and failure criterion predict that failure could occur over a broad range of values of the compressive load. The excellent test-analysis correlation obtained using the deterministic analysis is fortuitous. A highly accurate prediction of failure requires *both* an excellent mathematical model (including a valid failure criterion) and low variability of important parameters (including material properties, dimensions, support conditions, and loads).

This paper reinforces the need to account for uncertainties when carrying out structural analysis and design. Uncertainties cannot be eliminated, but they can be reduced by increasing quality control. Ideally, a properly-posed optimization problem for structural design should include the costs and benefits from various levels of quality control. The structure should be designed to minimize the total cost – including the cost of failure – while maintaining a prescribed reliability. Alternatively, the structure should be designed to maximize reliability without exceeding a prescribed total cost.

ACKNOWLEDGMENTS

The authors wish to express their appreciation to Susan L. McCleary, Lockheed Engineering & Sciences Co., who helped validate the finite element model for the second example, and to Bell Helicopter Textron – particularly to Robert V. Dompka – for providing technical data and photographs for the second example.

REFERENCES

Anderson, M. S.; Stroud, W. J.; Durling, B. J.; and Hennessy, K. W., 1980, "PASCO: Structural Panel Analysis and Sizing Code, Users Manual," NASA TM 80182.

Chamis, C. C., 1986, "Probabilistic Structural Analysis Methods for Space Propulsion System Components," Space System Technology Conference, San Diego, California, June 9-12, 1986, Technical Papers, AIAA, New York, pp. 133-144.

Davis, D. D., Jr., 1991, "Detailed Analysis and Test Correlation of a Stiffened Composite Wing Panel," NASA TM-104154.

Liu, W. K.; and Belytschko, T. (Editors), 1989, *Computational Mechanics of Probabilistic and Reliability Analysis*. Elmepress International, Lausanne, Switzerland.

Olesen, R, 1992, "PROBAN, General Purpose Probabilistic Analysis Program, User's Manual," Veritas Sesam Systems Report No. 92-7049, Veritas Sesam Systems (USA), Inc., Houston, TX 77077

Stewart, C. B. (Compiler), 1989, "The Computational Structural Mechanics Testbed User's Manual," NASA TM-100644.

Stroud, W. J.; Krishnamurthy, T.; Sykes, N. P.; and Elishakoff, I., 1992, "Effect of Bow-type Initial Imperfection on the Reliability of Minimum-Weight Stiffened Structural Panels," NASA TP-3263.

SwRI, 1991, "NESSUS Reference Manual, Version 1.0," Southwest Research Institute, San Antonio, TX 78228-0510.